Ab Initio Lattice Dynamics and Elastic Constants of ZrC

P.T. Jochym and K. Parlinski

Institute of Nuclear Physics, ul. Radzikowskiego 152, 31–342 Cracow, Poland

Abstract. *Ab initio* calculations and a direct method are applied to derive the phonon dispersion relations and phonon density of states for the ZrC crystal. The results are in good agreement with neutron scattering data. The force constants are determined from the Hellmann-Feynman forces induced by atomic displacements in a 2×2×2 supercell. The elastic constants are found using the deformation method and successfully compare with experimental data.

PACS. 63.20.–e Phonons in crystal lattices – 71.15.Mb Density functional theory

Studies of transition-metal carbides have been carried out several times. Phenomenological model calculations [1, 2,3] managed to reproduce the phonon dispersion relations quite well, but the interactions were quite sophisticated , some of them including three-body interactions and double shell models. Recently, there have been several studies based on *ab initio* methods[4,5,6,7]. The electronic structure, bulk modulus, and elastic constants, as well as the phonon dispersion relations have been found for TiC, TiN and TiO compounds by means of first-principles total-energy calculations [8,9]. Generally, the calculated values show good agreement with experiments. This provides a motivation to extend the investigation to heavier transition metals and to treat zirconium carbide, ZrC. This crystal is an important material in nuclear energy technology, since it provides a filling medium for fuel particles. It is also used for surface hardening and coverage of cathodes of X-ray sources. In this paper we continue to study the lattice dynamics and elastic properties of transition-metal compounds. See [8] and references given there for a more detailed description of the method.

The transition-metal carbide compounds, of which ZrC is a representative, are of considerable scientific and technological interest because of their striking mechanical properties, extreme hardness combined with metallic electrical and thermal conductivities. The ZrC crystal has NaCl structure and it is usually non-stoichiometric, mainly owing to carbon-vacancy defects. The phonon dispersion relations of ZrC have been measured along main symmetry directions by Smith et al [10,11]. Elastic constants, in turn, have been measured for two concentrations of carbon ($ZrC_{0.89}$ and $ZrC_{0.94}$) by Chang and Graham [12].

In this paper we extend the first-principle calculations to describe the phonon dispersion curves, phonon density and elastic constants of ZrC. The method which is used, is based on the total energy calculation and *Hellmann–*
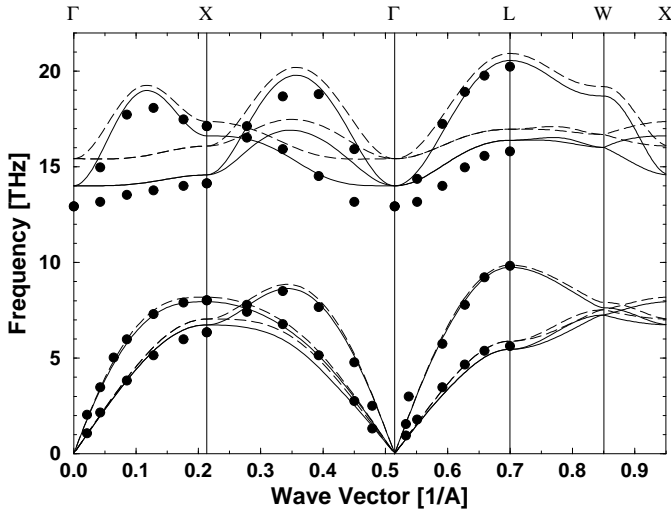
Feynman (HF) forces. The phonon dispersion relations are calculated by the *direct method* and the PHONON program [13,14,15,16,17,18], in which the force constants of the dynamical matrix are derived from HF forces. Alternatively, one could use the linear–response method [19, 20] for the evaluation of *ab initio* phonon frequencies at a predetermined set of Brillouin zone points. Elastic constants and bulk modulus are estimated by straightforward evaluation of energy derivatives with respect to the deformations.

The energies and HF forces of ZrC crystal are calculated by the method of total energy minimization, using norm-conserving *pseudopotentials* as an approximation for the atomic core–valence electron interaction [21,22,23]. This method allows to include the pressure in calculations as well as anharmonic effects. For the lattice dynamics calculations a 2×2×2 supercell with periodic boundary conditions and 64 atoms was used. For optimizing the structure and for the direct calculation of stress-strain relations a 1×1×1 supercell was utilized. The *ab initio* total energy calculations were done with the CASTEP package [24] and standard pseudopotentials constructed within LDA approximation and provided within this package. The Zr pseudopotential treats 4d electrons as belonging to the valence band. All pseudopotentials were parametrized in the reciprocal space with 680 eV cut–off energy.

Tests, which were made with the 1×1×1 supercell and with cut-off energies of 680 eV and 900 eV, showed that in the first case the cohesive energy is only 0.01 eV higher, and the lattice constant changes by only 0.0007 Å(0.01%). Therefore, we used the 680 eV cut-off energy for all remaining calculations.
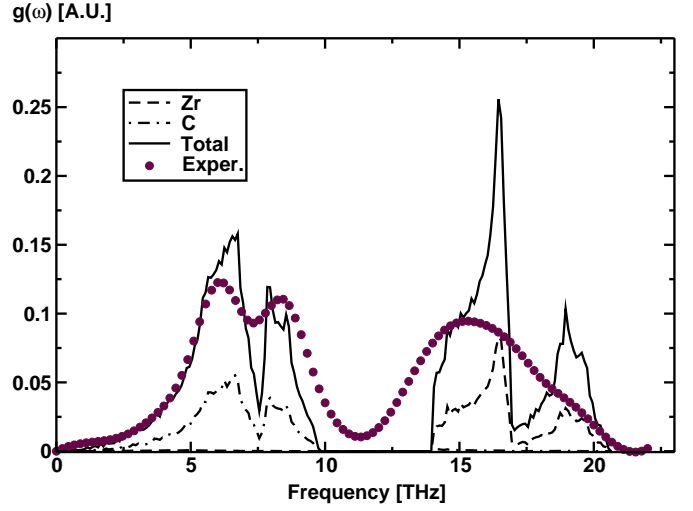
The *Local Density Approximation* (LDA) as well as the *Generalized Gradient Approximation* (GGA) were used for the exchange energy term of the valence states of the Hamiltonian [25]. The integration over the Brillouin zone was performed with weighted summation over wave vec-

tors generated by the Monkhorst-Pack scheme [26] using grid spacings from 0.1 Å^{-1} to 0.04 Å^{-1} which lead to sets of k-vectors containing from 4 to 118 wave vectors for the $1\times1\times1$ supercell and from 1 to 14 wave vectors for the $2\times2\times2$ supercell. The convergence of the force constants was achieved for grid spacing below 0.05 Å^{-1}. Hence, we carried on the optimization for a 0.05 Å^{-1} grid spacing, which leads to 32 and 4 k-points for the $1\times1\times1$ and the $2\times2\times2$ supercells, respectively. However, we used a 64 wave-vector set for the LDA calculation of the elastic constants. The metallic character of the TiC compound, studied in [8], indicated that the use of smearing does not substantially improve the quality of phonon dispersion relations. Thus, we did not use smearing in the case of ZrC. The use of non–metallic summation of the Brillouin zone is further justified by the fact that the electron density of states at the Fermi level is small for ZrC and similar compounds: TiC and HfC [1,27], and the related errors are of the same order as the errors of the DFT approach itself [8]. Namely, they are less then 0.05% for the lattice constant, less then 0.3% for the bulk modulus, and less then 5% for phonon frequencies.

Fig. 2. Phonon density of states $g(\omega)$ of the ZrC crystal and partial phonon density of states $g_{i,\alpha}(\omega)$, where α = C or Zr and $i = x$, y or z are the displacement directions. These are the GGA results. Experimental data taken from Ref. [28].

Fig. 1. Phonon dispersion relations of ZrC crystal calculated with a $2\times2\times2$ supercell within GGA (full line) and LDA (dashed line) approximations. The experimental points are taken from Ref. [10,11].

The minimization of the total energy leads to the equilibrium lattice constant of the stoichiometric ZrC $a =$ 4.691Å for LDA and $a = 4.695$Å for GGA. These values could be compared with the experimental values of $a =$ 4.6994Å for $ZrC_{0.94}$ and $a = 4.7004$Å for $ZrC_{0.89}$[12]. The phonon dispersion relations, which correspond to temperature T=0, are shown in Fig. 1. These are compared with experimental phonon frequencies measured by inelastic neutron scattering [10,11]. For GGA, the calculated force constants for all 10 coordination spheres of the $2\times2\times2$ supercell are presented in Table 1.

From Fig. 1 one sees that the experimental data at the Γ point are about $\Delta\omega = 0.05\omega$ lower than the calculated values. A reason for this could be that the experimental values are measured at room temperature and that anharmonic effects diminish the phonon frequencies. Another reason may relate to the non-stoichiometric concentration of carbon, which diminishes the average phonon frequencies as well. In other *ab-initio* calculations for alkali metals[13], graphite and diamond[14] the experimental phonon points also are at frequencies lower than calculated ones. On the same Fig. 1 we see the influence of the different exchange-correlation energy approximations on phonon frequencies. In this case, the LDA appears to be far less accurate than the GGA.

By sampling the dynamical matrix at many wave vectors, one can calculate the phonon density of states $g(\omega)$, and the partial phonon density of states $g_{x,Zr}(\omega)$ and $g_{x,C}(\omega)$. The $g(\omega)$ describes the number of phonon frequencies in an interval around ω, while $g_{x,Zr}$ and $g_{x,C}$ specify the number of phonon frequencies in an interval around ω, but only taking into account vibrations of Zr and C atoms, respectively. The density-of-state functions calculated from the GGA data are shown in Fig. 2. They are conventionally normalized to $\int g(\omega)d\omega = 1$ and $\int g_{x,\alpha}(\omega)d\omega = 1/6$, where α = Zr or C. The curves show that motions within acoustic dispersion curves are almost entirely due to Zr atoms. The sum of the zirconium density of states $(g_{x,Zr}(\omega)+g_{y,Zr}(\omega)+g_{z,Zr}(\omega))$ fits the total density of states $g(\omega)$ below 10 THz. The part of $g(\omega)$ above the gap is mainly due to vibrations of C atoms. Thus, ZrC forms quite a special crystal, in which the heavy Zr atoms, form a frame for the elastic motion, and the C atoms vibrate within the optical modes. We see in Table 1, that the magnitudes of the force constants between Zr–C and between Zr–Zr and C–C at a similar distance remain of the same order. Thus, ZrC does not consist of two weakly bounded subsystems. The situation is similar in TiC [8].

Distance (Å)	From	To	xx	yy	zz	yz	xz	xy
0.0	$C_{(0,0,0)}$	$C_{(0,0,0)}$	219.36	219.36	219.36			
0.0	$Zr_{(\frac{1}{2},\frac{1}{2},\frac{1}{2})}$	$Zr_{(\frac{1}{2},\frac{1}{2},\frac{1}{2})}$	284.67	284.67	284.67			
2.3447	$C_{(0,0,0)}$	$Zr_{(\frac{1}{2},0,0)}$	-24.20	-23.82	-23.82			
3.3159	$C_{(0,0,0)}$	$C_{(\frac{1}{2},\frac{1}{2},0)}$	-5.77	-5.77	0.64			-10.41
3.3159	$Zr_{(\frac{1}{2},\frac{1}{2},\frac{1}{2})}$	$Zr_{(1,1,\frac{1}{2})}$	-15.67	-15.67	-3.68			-31.66
4.0611	$C_{(0,0,0)}$	$Zr_{(\frac{1}{2},\frac{1}{2},\frac{1}{2})}$	-1.90	-1.90	-1.90	-1.20	-1.20	-1.20
4.6894	$C_{(0,0,0)}$	$C_{(1,0,0)}$	-21.97	1.02	1.02			
4.6894	$Zr_{(\frac{1}{2},\frac{1}{2},\frac{1}{2})}$	$Zr_{(1\frac{1}{2},\frac{1}{2},\frac{1}{2})}$	-17.47	3.82	3.82			
5.2429	$C_{(0,0,0)}$	$Zr_{(1,\frac{1}{2},0)}$	2.63	-0.01	0.53			
5.7433	$C_{(0,0,0)}$	$C_{(1,\frac{1}{2},\frac{1}{2})}$	0.37	0.36	0.36	-0.15	-0.02	-0.02
5.7433	$Zr_{(\frac{1}{2},\frac{1}{2},\frac{1}{2})}$	$Zr_{(1\frac{1}{2},1,1)}$	0.39	0.28	0.28	0.41		
6.6318	$C_{(0,0,0)}$	$C_{(1,1,0)}$	-0.94	-0.94	-0.05			
6.6318	$Zr_{(\frac{1}{2},\frac{1}{2},\frac{1}{2})}$	$Zr_{(1\frac{1}{2},1\frac{1}{2},\frac{1}{2})}$	0.52	0.52	-0.06			
7.0341	$C_{(0,0,0)}$	$Zr_{(1,1,\frac{1}{2})}$	-0.13	-0.13	-0.09			
8.1223	$C_{(0,0,0)}$	$C_{(1,1,1)}$	-0.03	-0.03	-0.03			
8.1223	$Zr_{(\frac{1}{2},\frac{1}{2},\frac{1}{2})}$	$Zr_{(1\frac{1}{2},1\frac{1}{2},1\frac{1}{2})}$	-0.01	-0.01	-0.01			

Table 1. Values of the non-zero elements of the force-constant matrices derived from a $2\times2\times2$ supercell in GGA (in N/m). All force-constant matrices are symmetric.

In Fig. 2 the experimentally determined phonon density of states taken from Ref.[28] is also shown. The agreement within the acoustic region is quite good. In the optical region the experimental resolution of ≈ 2.5 THz and the non-stoichiometry of carbon lead to considerable broadening.

Result	B	c_{11}	c_{12}	c_{44}
Expt $ZrC_{0.94}$ [10]	(2.231)	4.720	0.987	1.593
Expt $ZrC_{0.89}$ [10]	(2.225)	4.682	0.997	1.573
ZrC extrapolated	(2.238)	4.766	0.975	1.617
Calc. LDA	(2.270)	4.716	1.047	1.348
Calc. LDA (energ.)	2.295			
Calc. GGA	(2.279)	4.802	1.018	1.697
Calc. GGA (energ.)	2.32			

Table 2. Experimental and calculated bulk modulus B and elastic constants c_{ij} of the ZrC crystal, in units of $10^{11}\mathrm{Nm}^{-2} = 1\mathrm{MBar}$. Values in parentheses are calculated from $B = \frac{1}{3}(c_{11} + 2c_{12})$.

The bulk modulus was calculated in the $1\times1\times1$ supercell from the relation of pressure to the lattice constant. These data were fitted to a fourth order polynomial. Hence, the derivative $\partial P/\partial V$, and the bulk modulus B were calculated from the relation: $B = -V(\partial P/\partial V)$, where V is the volume of the ZrC crystallographic unit cell. For LDA and GGA, the B values are given in Table 2 and they agree quite well with experimental data. We also derived the bulk modulus from the energy-deformation relationship and the stress–strain relations, and the last proved to be more accurate than differentiation of the total energy curve (see Table 2).

We used stress–strain relations to obtain the elastic constants. The calculations of c_{11}, c_{12}, c_{44} elastic constants involved elongation and shear deformations. Deformations from 0.5% to 3% in length and from 1 to 5 degrees in angle are used. The results of small and large deformations are consistent. The deformed lattices have space groups Fm3̄m, I4/mmm and I/mmm, for bulk expansion, elongation along z, and shear modes, respectively. In all these deformed lattices all atoms remain in high-symmetry sites so that the relaxation of the internal degrees of freedom during the supercell deformations are not necessary. The calculated elastic constants are compared with the experimental data in Table 2. Generally they are in good agreement with experiments. The c_{12}, c_{44} elastic constants are better reproduced by the GGA, but also c_{11} fits better with GGA, when experimental data are extrapolated to the stoichiometric ZrC (third row in Table 2).

In summary, we have shown that the *ab initio* calculations of HF forces together with the direct method lead to a satisfactory description of phonons and elastic constants in the ZrC crystal. The phonon dispersion relations and the density of states fit well to neutron experimental data. The GGA offered better phonon frequencies and elastic constants.

References

1. W. Weber, Phys. Rev. B, **8**, 5082 (1973)
2. B.R.K. Gupta and M.P. Verma, J. Phys. Chem. Solids, **37** 815 (1976)
3. R.B. Yadav, Solid State Comm. **44** 1071 (1982)
4. A. Neckel, R. Eibler, P.Weinberger and K. Schwartz, J. Phys C **9**, 579 (1976).
5. V.P. Zhukov, V.A. Gubanov, O. Jepsen, N.E. Christensen and O.K. Andersen, J. Phys. Chem. Solids **49**, 841 (1988).
6. D.L. Price and B.R. Cooper, Phys. Rev. B **39**, 4945 (1989).
7. J. Häglund, A.F. Guillerment, G. Grimvall and M. Körling, Phys. Rev. B **48**, 11685 (1993).
8. P.T. Jochym, M. Sternik, K. Parlinski, Eur. Phys. J. B **10**, 9-13 (1999)
9. R. Ahuja, O. Eriksson, J. M. Wills, B. Johansson, Phys. Rev. B **53**, 3073 (1996).
10. H.G. Smith, in: *Superconductivity in d- and f-Band Metals*, Ed. D.H. Douglass, AIP, New York 1972.
11. H.G. Smith, N. Wakabayashi, R.M. Nicklow, S. Mihailovich, in: *Proc. 13th Internat. Conf. Low–Temperature Physics, Boulder (Col.) 1972*; Ed. R.H. Kropschot and K.D. Timmerhaus, University of Colorado Press, Boulder (Col.) 1973.
12. R. Chang and L.J. Graham, J. Appl. Phys. **37** 10 (1966) 3778
13. W.Frank, C.Elsässer, and M,Fähnle, Phys.Rev.Lett. **74**, 1791 (1995).
14. G.Kresse, J.Furthmüller, and J.Hafner, Europhys.Lett. **32**, 729 (1995).
15. K. Parlinski, Z. Q. Li and Y. Kawazoe, Phys. Rev. Lett. **78**, 4063 (1997).
16. G. J. Ackland, M. C. Warren and S. J. Clark, J. Phys.: Condens. Matter **9**, 7861–7872 (1997).
17. M.H.F. Sluiter, M. Weinert, Y. Kawazoe, Europhys. Lett. **43**, 183 (1998).
18. K. Parlinski, Phonon program (1999).
19. X. Gonze and J.P. Vigneron, Phys. Rev. B **39**, 13 120 (1989)
20. P. Giannozzi, S. de Gironcoli, P. Pavone, S. Baroni, Phys. Rev. B **43** 7231 (1991)
21. J.S. Lin, A. Qteish, M.C. Payne and V. Heine, Phys. Rev. B **47**, 4174 (1993).
22. J. Goniakowski, J.M. Holender, L.N. Kantorovich, M.J. Gillan and J.A. White, Phys. Rev. B **53**, 953 (1996).
23. M.C. Payene, M.P. Teter, D.C. Allan, T.A. Arias, J.D. Joannopoulos, Rev. of Mod. Phys. **64**, 1045 (1992)
24. CASTEP is a part of $Cerius^2$ system developed by Molecular Simulations.
25. J.P. Perdew, J.A. Chevary, S.H. Vosko, K.A. Jackson, M.R. Pederson, D.J. Singh, C. Fiolhais, Phys. Rev. B **46**, 6671 (1992).
26. H.J. Monkhorst and J.D. Pack, Phys. Rev. B **13**, 5188 (1976).
27. H. Bilz, Z. Phys. **153**, 338 (1958)
28. F. Gompf, J. Salgado, W. Reichardt, KFK-Report 2054 (1973/74), p. 21.